Erschienen in: Nature Neuroscience. Nature Publishing Group. 2013, 16(6), pp. 730-738
https://doi.org/10.1038/nn.3386

Object tracking in motion-blind flies

Armin Bahl, Georg Ammer, Tabea Schilling & Alexander Borst

Different visual features of an object, such as its position and direction of motion, are important elements for animal orientation, but the neural circuits extracting them are generally not well understood. We analyzed this problem in *Drosophila*, focusing on two well-studied behaviors known as optomotor response and fixation response. In the neural circuit controlling the optomotor response, columnar T4 and T5 cells are thought to be crucial. We found that blocking T4 and T5 cells resulted in a complete loss of the optomotor response. Nevertheless, these flies were still able to fixate a black bar, although at a reduced performance level. Further analysis revealed that flies in which T4 and T5 cells were blocked possess an intact position circuit that is implemented in parallel to the motion circuit; the optomotor response is exclusively controlled by the motion circuit, whereas the fixation response is supported by both the position and the motion circuit.

Optomotor and fixation responses of flies have been studied extensively. Experiments on tethered *Drosophila* walking or flying inside a rotating drum revealed a strong and persistent optomotor response along the direction of the rotating drum[1–3] (open loop). The effect of large-field stimuli on visual course control can also be seen in free flight, where the structure of the flight path of *Drosophila* depends on the visual pattern of the surrounding environment[4]. When the pattern is rotating, the fly's behavior exhibits distinct, circular flight paths around the center of the arena[5]. Fixation behavior was first observed in tethered flying house flies in which the fly's torque was fed back into a servo motor controlling the position of a black bar[6,7] (closed loop). Under these conditions, flies keep the bar in front of them most of the time. Moreover, it was shown that bar fixation interacts with the expansion avoidance reaction of *Drosophila* when presented with translatory full-field optic flow[8]. Fixation behavior has also been studied in freely walking and flying *Drosophila*[9–12]. On the basis of their different dynamics and spatial sensitivity, the optomotor and fixation responses were proposed to represent the output of different visual processing pathways[13]. Similar conclusions were drawn from experiments in which the tangential cells of the lobula plate were either genetically or surgically removed[14–17], or in mutants with reduced optic lobes[18]; in general, flies seem to be impaired more strongly in their response to large-field rotating patterns than in their reaction to single, moving bars. However, none of the techniques used provided a sufficiently high resolution to make any definitive statements about the involvement of individual cell types of the fly optic lobe in one or the other pathway.

To dissect the neural circuits underlying the optomotor and fixation responses, we built on recent progress in our understanding of the visual processing stream[19] leading from the photoreceptors R1–6 via lamina and medulla to directionally selective motion responses in the lobula plate tangential cells (LPTCs; **Fig. 1a**). Recording from LPTCs via whole-cell patch[20,21] combined with selective blockade of individual columnar cells revealed that lamina cells L1 and L2 provide the main input to the motion detection circuit, functionally segregating into an ON and an OFF pathway, respectively[22,23]. The L1 and L2 pathways, which have been described anatomically[24,25], converge again on the dendrites of the tangential cells in the lobula plate via T4 and T5 cells; blocking the synaptic output from T4 and T5 cells completely abolishes the motion response in tangential cells, but leaves some residual response to full-field flicker[26]. To test the behavioral performance of these flies, we used a procedure in which a tethered fly walks on a small sphere supported by an air stream[2,27]. A computer reads the movement of the sphere, controls the visual stimulus presented to the fly and adjusts the ambient temperature. Moreover, we used the *Gal4-UAS* system[28] to genetically express a temperature-sensitive allele of *shibire*[29] in a small subset of neurons in the fly brain. This permitted a selective shut down of the desired part of the neuronal circuit during the experiment by switching from the permissive temperature for *shibire^{ts}* (25 °C) to its restrictive one (34 °C).

RESULTS

Optomotor and fixation response

We tested the optomotor and fixation response of flies in which *shibire^{ts}* was expressed in T4 and T5 cells (T4/T5 block flies). As the behavior of flies turned out to be highly dependent on temperature (**Supplementary Fig. 1**), all of our control experiments were carried out with flies of a different genotype using the same temperature protocol. For controls, we used flies with two different genotypes: flies that carried the *shibire^{ts}* effector allele, but no *Gal4* driver gene (*shi^{ts}* control), and flies that carried the *Gal4* driver gene, but no *shibire^{ts}* effector gene (T4/T5 control). We examined the temperature dependency of the block: T4/T5 block flies behaved similar to control flies at 25 °C, as well as when the temperature was slowly elevated to 34 °C. However, clear differences emerged approximately 5 min after reaching 34 °C (**Supplementary Fig. 1**). To exclude any motor deficits in T4/T5 block flies, we analyzed their general walking and turning activity, which were not different from those of control flies (**Supplementary Fig. 2**).

Max Planck Institute of Neurobiology, Martinsried, Germany. Correspondence should be addressed to A. Bahl (bahl@neuro.mpg.de) or A. Borst (borst@neuro.mpg.de).

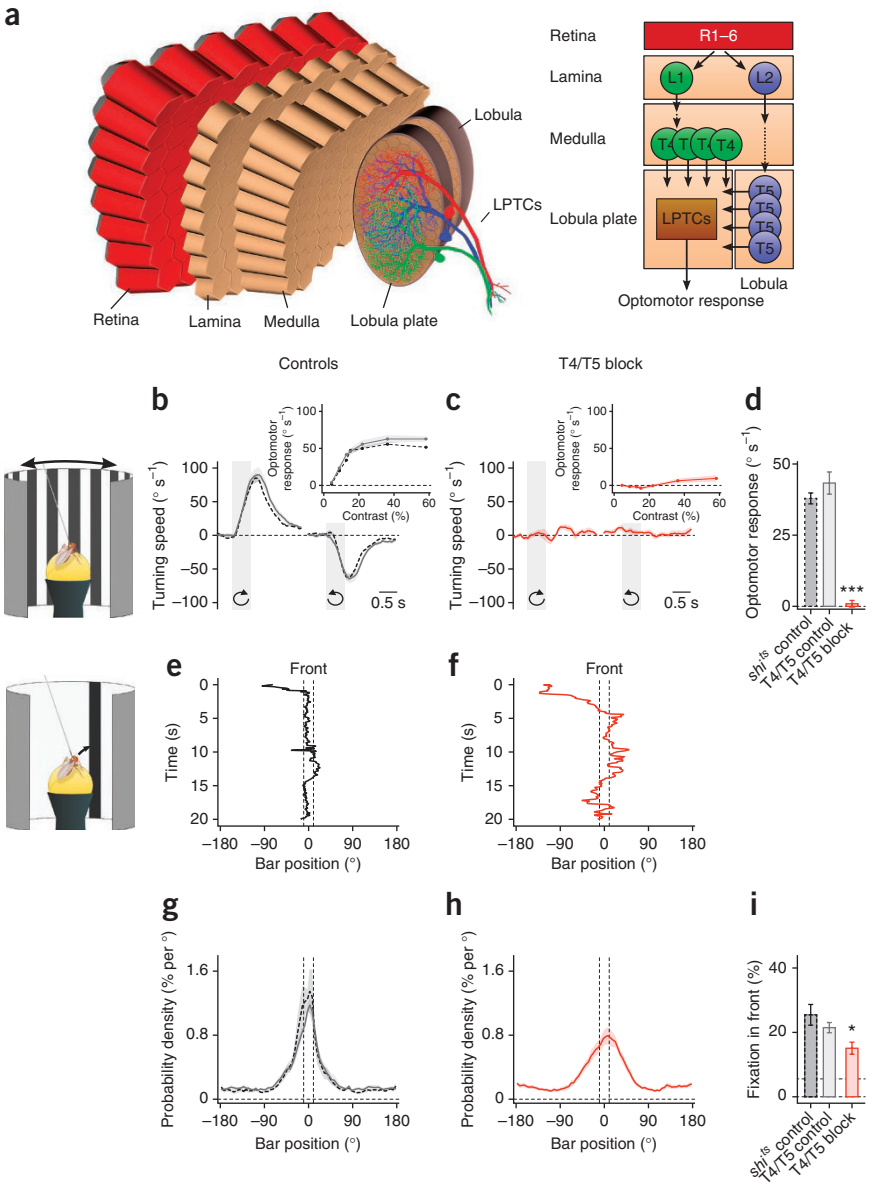

Figure 1 Optomotor response and fixation response of control and T4/T5 block flies. (**a**) Schematic of the fly's optic lobe. In each lamina column, photoreceptors R1–6 synapse onto lamina cells L1 and L2, forming parallel pathways for motion detection. The output signals of both pathways converge via T4 and T5 cells on the dendrites of LPTCs. (**b**,**c**) Turning speed of control (shi^{ts} control (dashed black line) and T4/T5 control (solid gray line); **b**) and T4/T5 block (solid red line; **c**) flies in response to clockwise and counterclockwise rotation of a grating pattern (contrast = 22%, gray shaded areas; 20 trials per fly, $n = 10$ flies per group). Inset, optomotor response as function of grating contrast (clockwise minus counterclockwise rotation response divided by 2; averaged in 1 s after stimulus onset). (**d**) Average optomotor response (average over contrasts). $^{***}P < 0.001$, two-sided t test compared with both control groups. The response of the T4/T5 block group was not significantly different from zero ($P = 0.47$, two-sided t test). (**e**,**f**) Bar position over time during closed-loop fixation (single trial of one shi^{ts} control fly (**e**), single trial for one T4/T5 block fly (**f**)). Vertical dashed lines indicate the frontal area (±10°). (**g**,**h**) Average probability density as function of bar position for control (40 trials per fly, $n = 10$ flies per group; **g**) and T4/T5 block (40 trials per fly, $n = 12$ flies; **h**) flies. (**i**) Integration of the probability density curves between ±10° gives the percentage of time the bar is held in the frontal visual field (fixation in front). Upper horizontal dashed line represents the chance level (5.6%, no fixation). $^{*}P < 0.05$, two-sided t test compared with both control groups. The value of the T4/T5 block group was significantly different from chance ($P < 0.001$, two-sided t test). All data represent mean ± s.e.m.

We first confronted the flies with a large-field grating moving clockwise and counterclockwise (**Fig. 1b–d**). Both types of control flies exhibited a strong and reliable optomotor response over a wide range of pattern contrasts (**Fig. 1b**,**d**). Instead, T4/T5 block flies no longer followed the motion of the panorama, no matter how high the pattern contrast (**Fig. 1c**,**d**). We next performed closed-loop fixation experiments and coupled the flies' turning tendency to the position of a single black bar such that whenever the fly turned into one direction, the bar moved into the other (**Fig. 1e–i**). Control flies robustly moved the bar to the front and kept it there (**Fig. 1e**,**g**,**i**). When we tested the flies in which the output from T4 and T5 cells was blocked, we were surprised that they were still clearly able to fixate the bar, although with a somewhat broader position distribution than control flies (**Fig. 1f**,**h**,**i**). Taken together, these results indicate that T4 and T5 cells are a necessary part of the neural circuit controlling the optomotor response to large-field motion, but are not needed for fixation behavior.

Dissection of motion and position system

Does that mean that fixation behavior relies on a separate set of motion-sensitive neurons tuned specifically to small moving objects, or does fixation behavior rely on a purely position-dependent system that is insensitive to motion? To tease apart the response to the direction and the response to the position of a moving bar, we used a classical approach[30] and moved a single bar in open loop around the fly, first in a clockwise and then in a counterclockwise direction, and measured both responses (R_{cw} and R_{ccw}, respectively) as a function of bar position (Ψ)[31].

Assuming that the turning response R of the fly to the rotating bar reflects a superposition of a position system P and a motion system M (with $v = d\Psi/dt$ denoting the angular velocity of the bar), we can write

$$R = P(\Psi, v) + M(\Psi, v)$$

For the two directions of bar rotations, we obtain

$$R_{cw} = P(\Psi, v) + M(\Psi, v)$$
$$R_{ccw} = P(\Psi, -v) + M(\Psi, -v)$$

To simplify these equations, two classical assumptions can be made[30]. First, the position system is velocity independent ($P(\Psi,v) = P(\Psi)$). Second, the motion system is linear in v ($M(\Psi,v) = M(\Psi)\cdot v$). Following

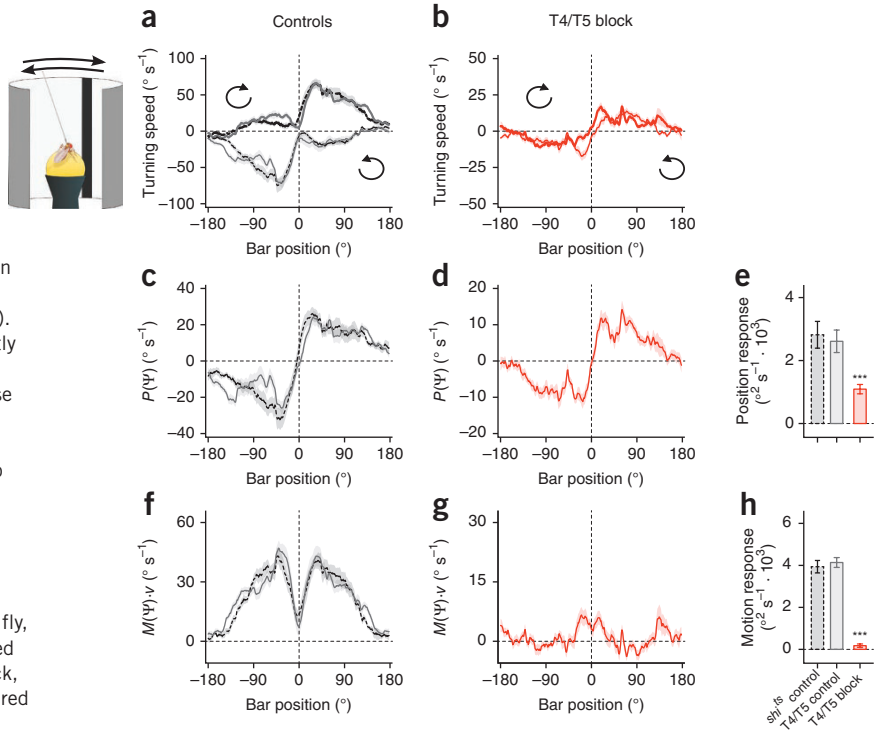

Figure 2 Open-loop analysis of the fixation response. (**a**,**b**) Responses of control (**a**) and T4/T5 block (**b**) flies to a single black bar moving clockwise (thicker lines) and counterclockwise around the fly. Responses are plotted as a function of the azimuth position of the bar; that is, during counterclockwise rotation, time progresses from right to left. (**c**,**d**) Summation of the clockwise and counterclockwise responses divided by 2 revealed the position-dependent response component, $P(\Psi)$, of control (**c**) and T4/T5 block (**d**) flies. (**e**) The position response (the integral of the curve $P(0° < \Psi < 180°)$ minus the integral of $P(-180° < \Psi < 0°)$ divided by 2). The response of the T4/T5 block group was significantly greater than zero ($P < 0.001$, two-sided t test). (**f**,**g**) Subtraction of the clockwise and counterclockwise responses divided by 2 yielded the motion-dependent response component, $M(\Psi)\cdot v$, of control (**f**) and T4/T5 block (**g**) flies (a positive value indicates a tendency to turn with the stimulus). (**h**) The motion response (the integral of the curve $M(0° < \Psi < 180°)\cdot v$ plus the integral of $M(-180° < \Psi < 0°)\cdot v$ divided by 2). The response of the T4/T5 block group was not significantly different than zero ($P = 0.06$, two-sided t test). All data represent mean ± s.e.m.; 35 trials per fly, $n = 10$, 11 and 14 flies per group (*shi*^{ts} control, dashed black lines; T4/T5 control, solid gray lines; T4/T5 block, solid red lines). $^{***}P < 0.001$, two-sided t test compared with both control groups.

these assumptions, the position system as well as the motion system can be recovered

$$P(\Psi) = (R_{cw} + R_{ccw})/2$$
$$M(\Psi)\cdot v = (R_{cw} - R_{ccw})/2$$

We performed such experiments on control and T4/T5 block flies (**Fig. 2**). With a starting position behind the flies, control flies followed the direction of motion of the bar, turning clockwise (+) during clockwise motion and counterclockwise (−) during counterclockwise motion (**Fig. 2a**), which is slightly different from what has been measured in flying *Drosophila* under similar conditions[8]. According to the formal decomposition outlined above, we recovered a position-dependent response component, $P(\Psi)$ (**Fig. 2c**,**e**), and a motion-dependent response component, $M(\Psi)$ (**Fig. 2f**,**h**). The responses of T4/T5 block flies to such stimuli were markedly different from those of control flies; in general, T4/T5 block fly responses had smaller amplitudes and were almost identical for both directions of bar motion (**Fig. 2b**). Decomposing the reaction into the position- and motion-dependent components revealed that the response of these flies to the position of the bar, $P(\Psi)$, was still present, although reduced in amplitude (**Fig. 2d**,**e**). However, the response to the motion of the moving bar, $M(\Psi)$, was completely abolished (**Fig. 2g**,**h**). We conclude that T4/T5 block flies are blind to the motion of a single bar, but can still detect its position. Thus, the ability of motion-blind flies to fixate a bar in closed loop (**Fig. 1f**,**h**,**i**) is a result of the remaining position response.

What is the visual cue used by the position system that allows the detection of bar position: is it mere stationary contrast, its temporal change or its local motion? To address these questions, we presented control flies with an appearing black bar (10° width) at +90° azimuth which stayed there for 4 s before disappearing again (**Fig. 3**). The time during which the bar appeared and disappeared amounted to 0.5 s approximating the local luminance change when a black bar (width = 10° and $v = 20\ ° s^{-1}$) moves into a 10°-wide window and, after 4 s, moves out again. Control flies exhibited a strong, but transient, response toward the position at which the bar was appearing as well as where it was disappearing, but, during the stationary phase of the bar, no response was detectable (**Fig. 3a**). We then determined the response values as function of bar position. In control flies, the shape of the resulting response functions (**Fig. 3c**,**i**) looked similar to $P(\Psi)$ as obtained in the previous experiment (**Fig. 2c**,**d**). We next repeated the experiments on T4/T5 block flies. Like control flies, T4/T5 block flies responded transiently to both the appearance as well as to the disappearance of the bar, but not when the bar was stationary (**Fig. 3b**). Moreover, the shape of the position-dependent response functions was almost identical to the ones of control flies (**Fig. 3d**,**g**,**j**). We conclude that the position system is insensitive to a stationary image but uses the change of luminance over time as its input signal[32]. Furthermore, the position system is not affected by blocking the output of T4 and T5 cells.

Turning responses to local motion and luminance changes

We observed a clear reduction of the performance of T4/T5 block flies compared to controls when we characterized their position response under closed-loop fixation conditions (**Fig. 1e**–**i**) and when we used a rotating bar (**Fig. 2**). However when we used local luminance changes, we found no difference between T4/T5 block and control flies (**Fig. 3**). This discrepancy suggests that the detection of motion somehow enhances the fly's response toward the position of the bar. We considered two possible mechanisms. First, the motion and position system may not be fully separable on the neuronal level. In this case, local motion might directly modify the position system to enhance the position response. Second, the motion system may have a stronger response to front-to-back than back-to-front motion. In the behaving fly, this would lead to a stronger compensation of bar motion away from the front, thereby improving fixation[33]. In both cases, T4/T5 block flies would no longer be able to detect the motion of the bar and their position response would be reduced. Furthermore, both arguments indicate that our assumptions (**Fig. 2**), which were adopted from classical experiments[30], might not be fully correct.

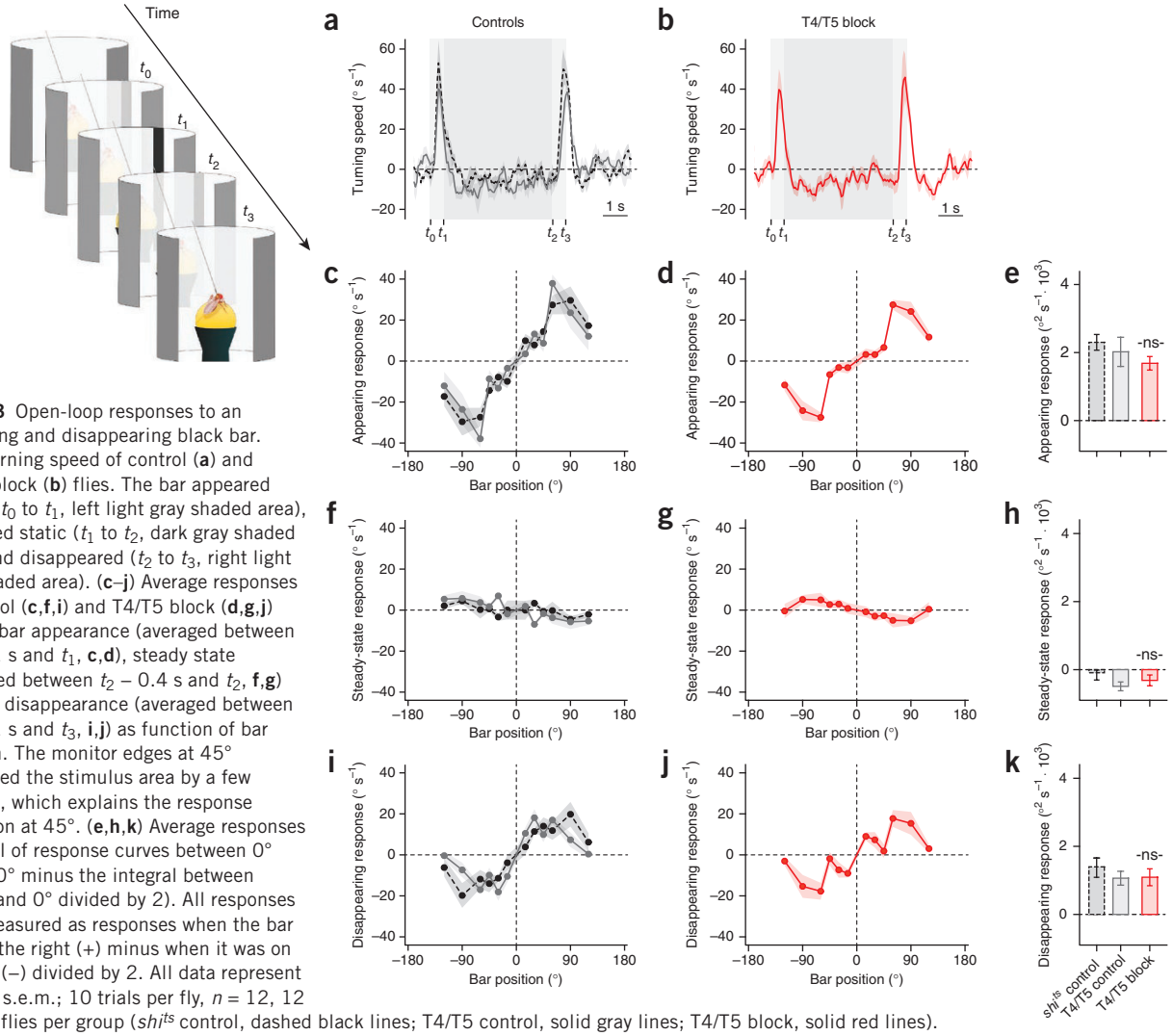

Figure 3 Open-loop responses to an appearing and disappearing black bar. (**a**,**b**) Turning speed of control (**a**) and T4/T5 block (**b**) flies. The bar appeared at 90° (t_0 to t_1, left light gray shaded area), remained static (t_1 to t_2, dark gray shaded area) and disappeared (t_2 to t_3, right light gray shaded area). (**c**–**j**) Average responses of control (**c**,**f**,**i**) and T4/T5 block (**d**,**g**,**j**) flies to bar appearance (averaged between t_0 + 0.1 s and t_1, **c**,**d**), steady state (averaged between t_2 – 0.4 s and t_2, **f**,**g**) and bar disappearance (averaged between t_2 + 0.1 s and t_3, **i**,**j**) as function of bar position. The monitor edges at 45° decreased the stimulus area by a few degrees, which explains the response reduction at 45°. (**e**,**h**,**k**) Average responses (integral of response curves between 0° and 120° minus the integral between −120° and 0° divided by 2). All responses were measured as responses when the bar was on the right (+) minus when it was on the left (–) divided by 2. All data represent mean ± s.e.m.; 10 trials per fly, n = 12, 12 and 16 flies per group (*shi^{ts}* control, dashed black lines; T4/T5 control, solid gray lines; T4/T5 block, solid red lines). ns indicates not significant, $P \geq 0.05$, two-sided t test compared with both control groups. Responses of T4/T5 block flies at 45° were not significantly different to control responses ($P \geq 0.05$; two-sided t test compared with both control groups). Responses of *shi^{ts}* control and T4/T5 block flies during steady state were not significantly different from zero, but the response of T4/T5 control flies was (P = 0.37, 0.11, 0.02, respectively; two-sided t test).

To test these ideas, we investigated the turning responses to local front-to-back motion, back-to-front motion and luminance changes in isolation (**Fig. 4**). We created a virtual environment consisting of a gray cylinder with a 10° window at two azimuthal positions (either Ψ = 30° or Ψ = 60°). Outside, a 10° black bar rotates at 40 ° s^{-1} around the cylinder. Whenever the bar passes the window, it briefly allows the fly's motion system to detect the direction of bar motion (either front to back or back to front), inducing a turning tendency (M_{FTB} and M_{BTF}) in the same direction. Moreover, when the bar passes through the window, it produces local luminance changes such that luminance first decreases and then increases again. This change in luminance is detected by the fly's position system, leading to an additional turning tendency toward that position (P_{FTB} and P_{BTF}). Thus, the turning response to local front-to-back and back-to-front motion can be described as the sum of both turning tendencies.

$$R_{FTB} = M_{FTB} + P_{FTB}$$
$$R_{BTF} = M_{BTF} + P_{BTF}$$

To tease apart the different response components, we need the response of the position system alone. We approximated the local luminance change when the rotating bar passes the window with a non-moving stimulus. The whole window starts at background luminance, darkens and then brightens again. This stimulus should only activate the position system, resulting in a turning tendency toward the position of the local luminance change ($R_L = P_L$).

When measuring the turning response of control flies to the three different stimulus conditions, all turning responses were found to be different. The response to the front-to-back stimulus (R_{FTB}) was positive and large in amplitude (**Fig. 4a**,**c**), the response to the back-to-front stimulus (R_{BTF}) was biphasic and weak (**Fig. 4d**,**f**), and the response to local luminance changes (R_L) was positive and weak (**Fig. 4g**,**i**). In contrast, the responses of T4/T5 block flies to front-to-back motion, back-to-front motion and local luminance changes were all identical (**Fig. 4b**,**e**,**h**,**j**). We found no differences in the responses to local luminance changes of controls and T4/T5 block flies (**Fig. 4i**), which is consistent with our earlier observations (**Fig. 3**). Taken together, these results indicate that the position system only detects changes in local luminance and that local motion does not influence its response properties. Thus,

$$R_L = P_L = P_{FTB} = P_{BTF}$$

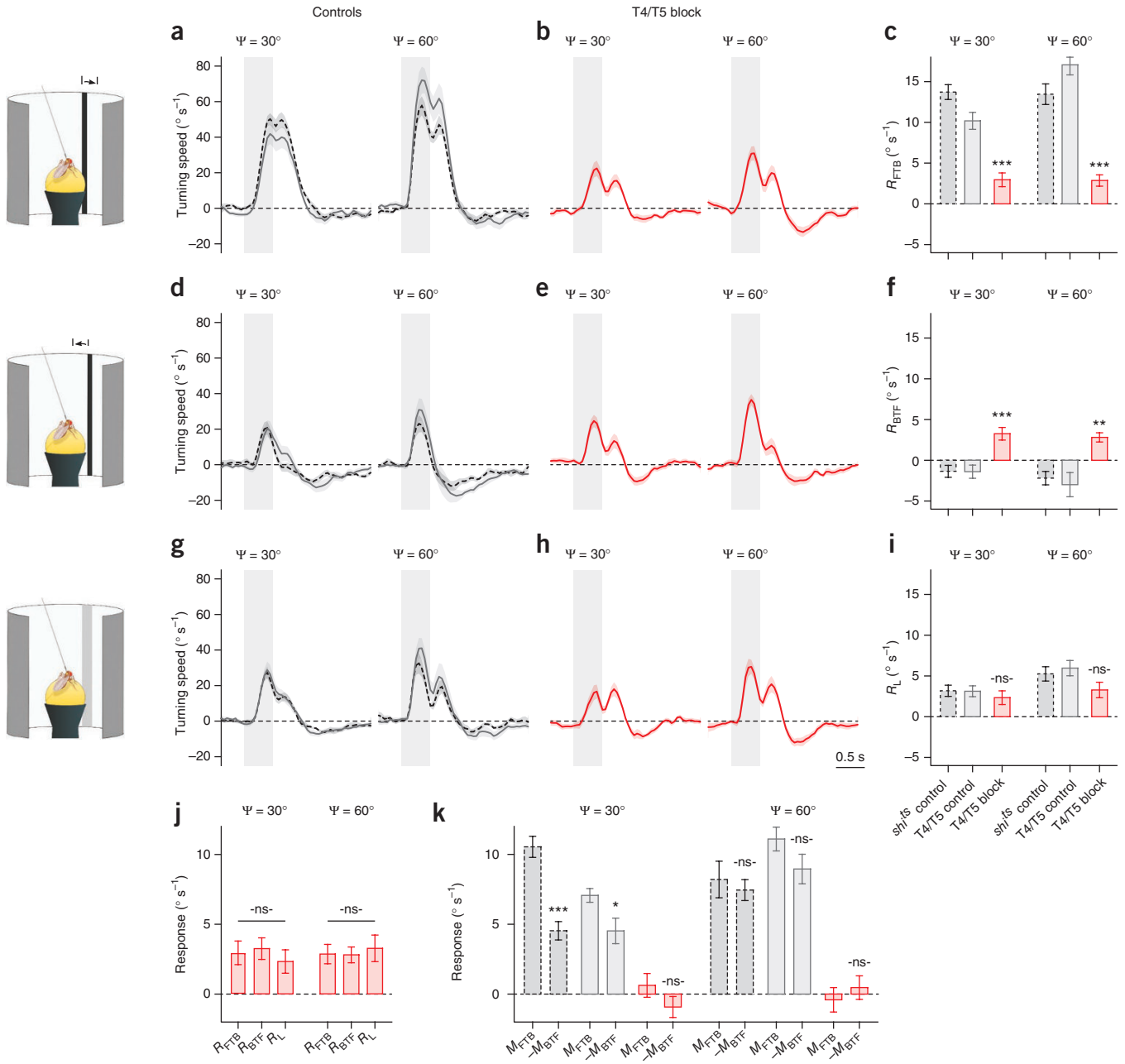

Figure 4 Open-loop responses to local bar motion and to local luminance changes. (**a**–**i**) Turning responses of control (**a**,**d**,**g**) and T4/T5 block (**b**,**e**,**h**) flies to local front-to-back motion (**a**,**b**), local back-to-front motion (**d**,**e**) and local luminance changes (**g**,**h**) at $\Psi = 30°$ and $\Psi = 60°$ (gray shaded areas). The corresponding average turning responses are shown in **c**, **f** and **i** (R_{FTB}, R_{BTF} and R_L, respectively; averaged between $t = 0.1$ s and $t = 2.1$ s after stimulus onset). (**j**) Comparison of responses to the different stimuli of T4/T5 block flies. (**k**) Comparison of isolated motion responses ($M_{FTB} = R_{FTB} - R_L$ and $M_{BTF} = R_{BTF} - R_L$). Motion responses of T4/T5 block flies were not significantly different from zero ($P \geq 0.05$, two-sided t test). All responses were measured as the response with the bar at $\Psi = +30°$ or $\Psi = +60°$ minus the response with the bar at $\Psi = -30°$ or $\Psi = -60°$, respectively, divided by 2. All data represent mean ± s.e.m.; 60 trials per fly of $n = 10$, 12 and 11 flies (at $\Psi = 30°$) and of $n = 10$, 11 and 11 flies (at $\Psi = 60°$) per group (shi^{ts} control, dashed black lines; T4/T5 control, solid gray lines; T4/T5 block, solid red lines). ns indicates not significant ($P \geq 0.05$), $^*P < 0.05$, $^{**}P < 0.01$ and $^{***}P < 0.001$; two-sided t-test compared with both controls (**c**,**f**,**i**) or comparing M_{FTB} to $-M_{BTF}$ within the groups (**k**); one-way ANOVA in **j**.

This finding allowed us to isolate the responses of the motion system to front-to-back and back-to-front stimulation.

$$M_{FTB} = R_{FTB} - R_L$$
$$M_{BTF} = R_{BTF} - R_L$$

Analyzing the data of control flies in this way revealed a strong asymmetry in the motion system for the frontal part of the visual field ($\Psi = 30°$), where its response to front-to-back was approximately twice as strong as that to back-to-front motion (**Fig. 4k**). In the lateral part ($\Psi = 60°$), we observed a similar tendency (**Fig. 4k**). This finding implies that $M(\Psi, v) \neq -M(\Psi, -v)$ and suggests that it is

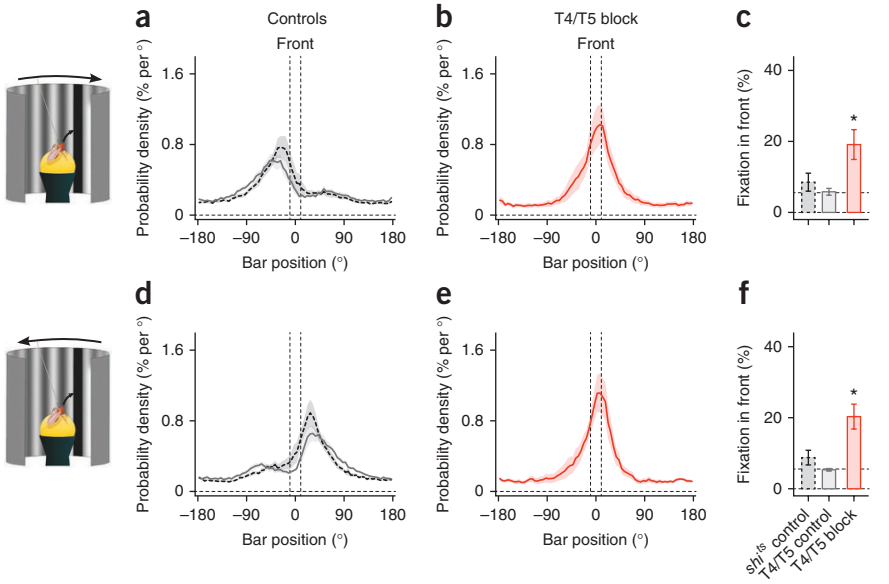

Figure 5 Closed-loop fixation response during open-loop background motion. (**a**–**f**) Fixation responses of control (**a**,**d**) and T4/T5 block (**b**,**e**) flies during clockwise (**a**,**b**) and counterclockwise (**d**,**e**) rotation of the sine-grating. The ability to keep the bar in front is shown in **c** and **f** (same measure as in **Fig. 1i**). Upper horizontal dashed lines represent the chance level (5.6%, no fixation). All data represent mean ± s.e.m.; 30 trials of $n = 11$, 9 and 9 flies per group (shi^{ts} control, dashed black lines; T4/T5 control, solid gray lines; T4/T5 block, solid red lines). $^*P < 0.05$, two-sided t test compared with both controls.

necessary to omit the classical assumption of velocity linearity of the motion system[30]. Consequently, we revised the interpretation of $P(\Psi)$ obtained in the previous experiment with the rotating bar (**Fig. 2**). Thus, $P(\Psi)$ actually overestimates the response of the pure position system (P_L) in control flies.

$$\begin{aligned} P(\Psi)^{\text{controls}} &= (R_{cw} + R_{ccw})/2 \\ &= (M(\Psi, v) + M(\Psi, -v) + 2 \cdot P_L)/2 \\ &> P_L \end{aligned}$$

On the other hand, for T4/T5 block flies, the motion responses were zero (**Figs. 2h** and **4k**). Under these conditions, $P(\Psi)$ corresponds to the response of the position system alone (P_L).

$$\begin{aligned} P(\Psi)^{\text{T4/T5 block}} &= (R_{cw} + R_{ccw})/2 \\ &= (M(\Psi, v) + M(\Psi, -v) + 2 \cdot P_L)/2 \\ &= P_L \end{aligned}$$

Taken together, these results indicate that the visual pathways of the motion and position system are indeed separable at the neuronal level. However, fixation is shaped by an interaction of both systems at the level of behavior.

Object tracking with background motion

Do both control systems also superimpose when the fly encounters a more natural situation where it has to track an object while the whole background is in motion? To answer this question, we fed back the fly's turning tendency on the position of the black bar, as in the usual fixation procedure (closed loop), and displayed a large-field sine-grating rotating in one or the other direction without giving the fly control over it (open loop) (**Fig. 5**). If both responses superimpose at the level of the fly's turning tendency, the large field stimulus should create a permanent offset, leading to a shift of the position where the fly fixates the bar.

We tested whether the presence of the sine-grating alone would alter the fixation response. To our surprise, the fixation response clearly improved for both control and T4/T5 block flies when the background was a static sine-grating (**Supplementary Fig. 3**), although the grating had the same average luminance as the uniformly gray background used in previous fixation experiments (**Fig. 1e**–**i**). This indicates that the fixation response is modulated by the spatial properties of the background, yet the detailed mechanism of this effect remains unknown.

With the sine-grating background moving clockwise or counterclockwise, control flies were still able to fixate the bar, but the peak of the position histogram was shifted in the direction opposite to the direction of the moving large-field stimulus (**Fig. 5a**,**d**). The motion system produced a tendency to turn in the direction of the moving background, whereas the position system induced turning toward the position of the bar. When the bar was shifted opposite to the direction of background motion, both responses summed to zero. Under the same conditions, T4/T5 block flies did not shift the fixation peak, but rather kept the bar in front of them, regardless of whether the large-field stimulus was moving clockwise or counterclockwise (**Fig. 5b**,**e**). These results suggest a superposition of the large-field motion system and the position system at the level of behavioral output, as has been proposed[30].

Electrophysiology in horizontal and vertical system cells

In our behavioral experiments, we found that a turning response could be elicited by local luminance changes and that this response was not changed when blocking T4 and T5 cell output (**Figs. 3** and **4**). In electrophysiological recordings from LPTCs sensitive to horizontal and vertical motion (horizontal and vertical system cells, respectively), the response to full-field flicker is only moderately reduced when T4 and T5 cell output is blocked[26], indicating that horizontal system and vertical system cells receive additional input from an unidentified flicker pathway. To investigate whether horizontal system or vertical system cells use this information to mediate the position response, we performed electrophysiological recordings from horizontal system and vertical system cells in the immobilized fly (**Fig. 6**). We presented gratings moving in different directions, full-field OFF and ON flicker, as well as appearing and disappearing black bars at different positions along the azimuth. Vertical system cells responded strongly in a direction-selective manner to vertical motion (**Fig. 6a**), whereas horizontal system cells responded most strongly to horizontal motion (**Fig. 6b**). Both cell types also responded strongly to full-field OFF and ON flicker. However, cellular responses to appearing and disappearing vertical bars were orders of magnitude weaker. Moreover, horizontal system cells slightly hyperpolarized when the black bar appeared, but depolarized when it disappeared.

These recordings conflict with the behavioral responses that we observed in several ways. First, flies robustly turned toward the

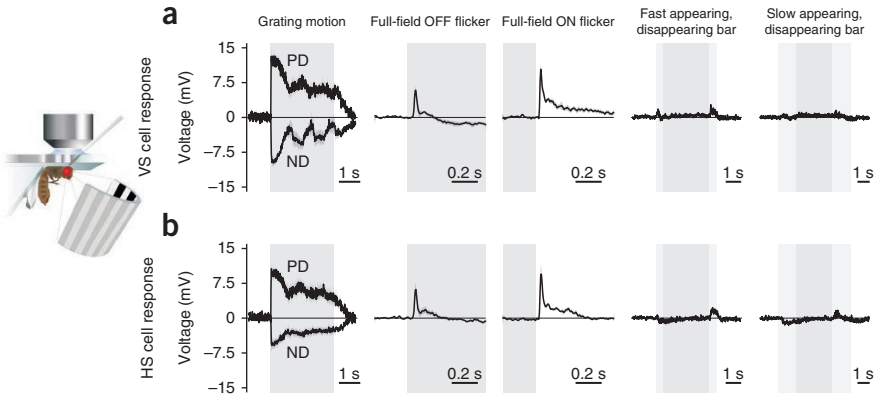

Figure 6 *In vivo* electrophysiological recordings from vertical system (VS) and horizontal system (HS) cells in the immobilized fly. (**a**,**b**) Voltage traces obtained from vertical system (**a**) and horizontal system cells (**b**) while presenting vertical (**a**) or horizontal (**b**) grating motion into the preferred direction (PD) and the null direction (ND) of the cell, full-field OFF and ON flicker, and a vertical dark bar that appeared and disappeared (fast or slow in 0.5 s or 1.5 s, respectively) at $\Psi = 30°$ in the front of the fly (responses at $\Psi = 60°$ and $\Psi = 90°$ were similar in amplitude; data not shown). All data represent mean ± s.e.m. obtained from $n = 8$ vertical system cells and $n = 6$ horizontal system cells from wild-type Canton S flies.

location of an appearing and a disappearing black bar, and this position response was on the same order of magnitude as the optomotor response to full-field grating motion (**Figs. 1b** and **3a**). Second, assuming that horizontal system and vertical system cells convey position information, we would not expect the fly to remain capable of tracking objects when the background is moving (**Fig. 5**); the tiny voltage responses to local luminance changes would vanish in the much stronger voltage response to the background motion. These discrepancies between electrophysiological responses of horizontal system and vertical system cells and behavioral responses render it unlikely that horizontal system and vertical system cells are part of the fly's position circuit.

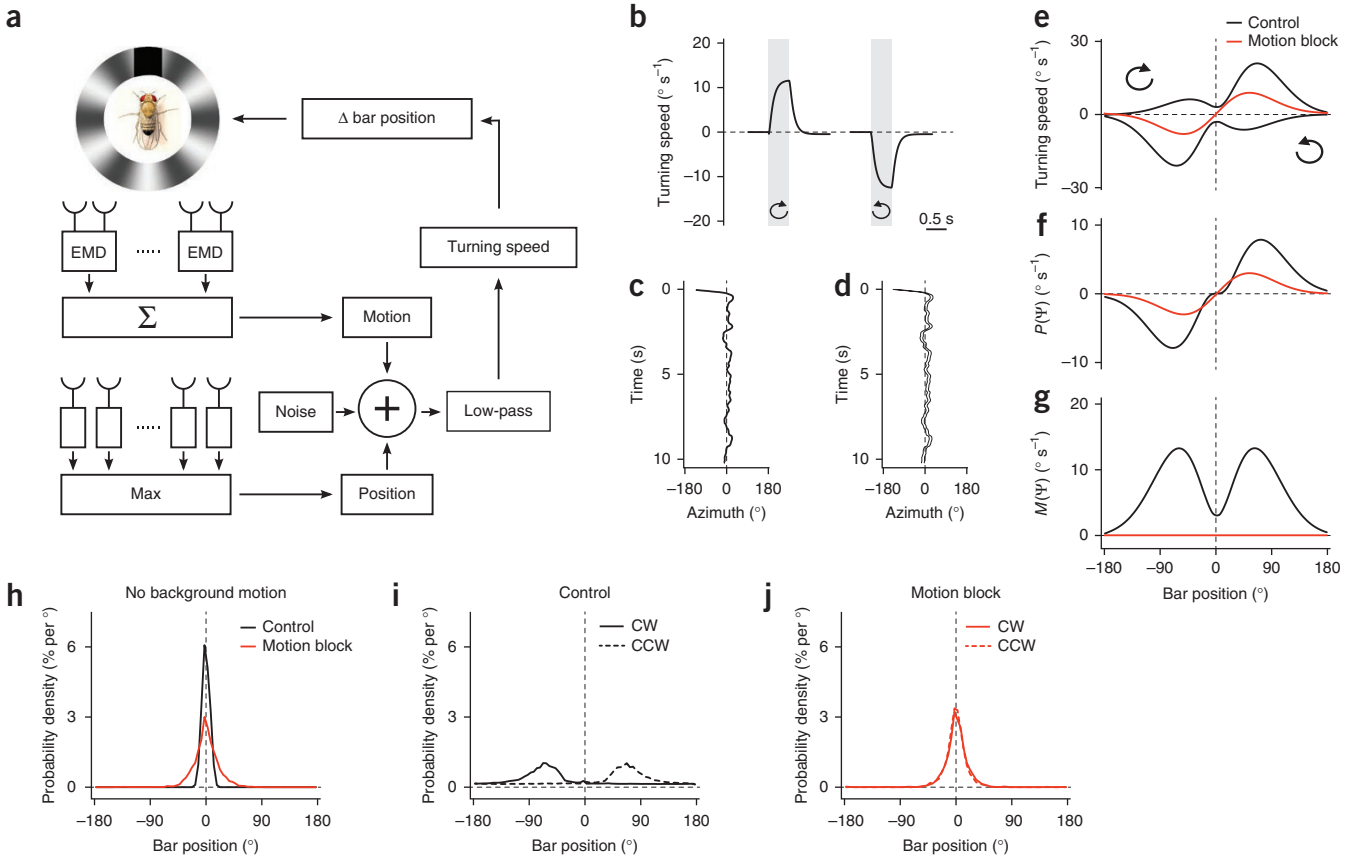

Figure 7 Model simulations of the fly's course control system. (**a**) Outline of the model. The visual scene was analyzed in parallel by a motion and a position system. Their output signals, plus noise, were summated and low-pass filtered to yield the fly's turning speed. To simulate closed-loop fixation behavior, this signal was used to control the bar position. (**b**) Turning responses of the model to full-field clockwise and counterclockwise grating rotation. (**c**,**d**) Bar position over time (**c**) and the resulting activity pattern of the array of position detectors (**d**) during a single run of closed-loop fixation. (**e**) Model responses to a bar rotating in open-loop clockwise, followed by counterclockwise. (**f**) Position component, $P(\Psi)$ (calculated by summing the two responses obtained in **e** and dividing them by 2). (**g**) Motion component, $M(\Psi)$ (calculated by subtracting the two responses obtained in **e** and dividing by 2). (**h**) Probability density as function of bar position obtained from 20 runs of closed-loop bar fixation. (**i**,**j**) Closed-loop fixation behavior during superimposed open-loop background sine-grating motion (solid lines, 10 ° s^{-1} clockwise (CW) rotation of the grating; dashed lines, −10 ° s^{-1} counterclockwise (CCW) rotation of the grating). Model responses were calculated with an intact motion system (black lines) and with the gain of the motion system set to zero (red lines).

Modeling

Our results suggest the existence of two course control systems operating in parallel. Can such a system track a single object effectively and quantitatively account for the observed behavior of the flies? To address this question, we modeled the two course control systems and tested them under the conditions that were used in the experiments (**Fig. 7**). We implemented the large-field motion system as an array of elementary motion detectors of the Reichardt type[34] weighted by a spatial sensitivity profile similar to $M(\Psi)$, as obtained in the experiments (**Fig. 2f**), and with a 50% stronger weight on front-to-back than on back-to-front motion, as we observed (**Fig. 4k**). The output signals of all motion detectors were summated. The position system was modeled as an array of squared high-pass filters. From the array, the location of the maximum response was extracted at each time point. The response amplitude toward this position was determined from a spatial sensitivity profile similar to the experimentally determined one (**Fig. 2c**,**d**). Both signals were multiplied by a gain factor, added together with white noise and low-pass filtered to obtain a turning signal. This could either be interpreted as the output signal under open-loop conditions or fed back into the bar position when simulating closed-loop fixation behavior (**Fig. 7a**).

Stimulating the model with grating motion under open-loop conditions resulted in a syndirectional optomotor response (**Fig. 7b**). When tested under closed-loop conditions, the model revealed a pronounced fixation behavior, bringing and keeping the bar in a frontal position (**Fig. 7c**,**h**). Comparing the bar position (**Fig. 7c**) with the output of the squared high-pass filters over time (**Fig. 7d**) revealed the effective detection of bar position. Moving the bar in open loop, first clockwise, then counterclockwise, led to a response profile that was consistent with the respective experimental data (**Fig. 7e**). We added and subtracted both responses to reveal the position-dependent and motion-dependent components ($P(\Psi)$ and $M(\Psi)$, respectively) and obtained similar profiles as in our experiments (**Fig. 7f**,**g**). We then tested the system for closed-loop fixation during open-loop background grating motion. As seen in the experiments, the maximum of the fixation histograms moved opposite to the direction of the drifting grating and the histograms became broader (**Fig. 7i**).

We then tested the model with the gain of the large-field motion system set to zero, simulating the blockage of T4 and T5 cell output; the model was still able to keep the bar in front, yet with a broader distribution (**Fig. 7h**). When the model was presented with the clockwise and counterclockwise rotating bar, the responses were identical for both directions of bar motion and only depended on the bar's position (**Fig. 7e**). Moreover, the resulting position-dependent response function, $P(\Psi)$, was reduced in amplitude compared with the control (**Fig. 7f**). Finally, in the case of closed-loop fixation with background motion, the model kept the bar in front, no matter the direction in which the background was moving (**Fig. 7j**). In summary, all of the effects that we observed in the experiments were reproduced by the model with one set of parameters.

DISCUSSION

Behavioral and electrophysiological studies in larger fly species have proposed that fixation behavior is mediated by a special class of lobula plate neurons that are selective for small moving objects[35–38]. These cells are thought to receive retinotopic input from the same set of columnar, motion-sensitive neurons as the large field–sensitive tangential cells. Their selectivity for small moving objects arises from additional inhibition that they receive from other large-field neurons of the lobula plate[39–41]. In contrast, we found that transgenic *Drosophila* in which the T4 and T5 cells were blocked were still able to fixate and track individual objects, even though their lobula plate tangential cells were motion blind and flies consequently did not show an optomotor response[26]. Our genetic and behavioral experiments revealed a control system that is purely sensitive to the position of the object and not to the direction in which it is moving, with the exact same spatial sensitivity profile as that revealed by the mathematical examination of behavioral results in wild-type houseflies performed many years ago[30]. Although the reduction in fixation strength observed in T4/T5 block flies might, at first sight, be interpreted as a partial overlap between the motion and the position circuit at the neuronal level, our analysis indicates that this is not the case; as a result of its asymmetry with respect to the direction of motion (front to back as compared to back to front), the motion circuit contributes to the fixation response at the behavioral level, but is separate from the position circuit at the neuronal level. An asymmetry in turning was also observed in the responses to rotating stripes[8,30] (**Fig. 2**), but, from these findings, one cannot conclude that the response of the motion circuit is asymmetrical. Even a perfectly symmetrical motion response, combined with the position response, would lead to the very same behavior. Our investigation of the two response components revealed that the asymmetrical turning response has two sources: a turning response to the position of the rotating bar and an asymmetrical motion response to its direction of motion. The powerful genetic tools available in *Drosophila*[42] will allow the future identification of the specific neural components of the position circuit.

METHODS

Methods and any associated references are available in the online version of the paper.

ACKNOWLEDGMENTS

We wish to thank G. Rubin and A. Nern for providing the T4/T5 cell–specific driver line *R42F06-Gal4* and V. Jayaraman for advice on setting up the locomotion recorder. We are also grateful to J. Haag, A. Mauss, A. Arenz and A. Leonhardt for many helpful discussions and critically reading the manuscript, S. Prech for help with the design of the Peltier temperature control system, C. Theile for fly work, and F. Foerstner for reconstructing the three horizontal system cells shown in **Figure 1a**. A. Bahl and A. Borst are members of the Bernstein Center for Computational Neuroscience and the Graduate School of Systemic Neurosciences.

AUTHOR CONTRIBUTIONS

A. Bahl set up the locomotion recorder and the stimulus display, and wrote the software for reading the behavioral output and displaying the stimulus. A. Bahl and T.S. performed all of the behavioral experiments and evaluated the data. G.A. performed the electrophysiological recordings and analyzed the data. A. Bahl and A. Borst designed the study. A. Borst carried out the modeling work. A. Borst and A. Bahl wrote the manuscript with the help of the other authors.

COMPETING FINANCIAL INTERESTS

The authors declare no competing financial interests.

1. Götz, K.G. Optomotorische Untersuchung des visuellen Systems einiger Augenmutanten der Fruchtfliege *Drosophila*. *Kybernetik* **2**, 77–92 (1964).
2. Buchner, E. Elementary movement detectors in an insect visual system. *Biol. Cybern.* **24**, 85–101 (1976).
3. Blondeau, J. & Heisenberg, M. The three-dimensional optomotor torque system of *Drosophila melanogaster*. Studies on wild type and the mutant optomotor blind H31. *J. Comp. Physiol. A* **145**, 321–329 (1982).
4. Tammero, L.F. & Dickinson, M.H. The influence of visual landscape on the free flight behavior of the fruit fly *Drosophila melanogaster*. *J. Exp. Biol.* **205**, 327–343 (2002).

5. Mronz, M. & Lehmann, F.-O. The free-flight response of *Drosophila* to motion of the visual environment. *J. Exp. Biol.* **211**, 2026–2045 (2008).
6. Reichardt, W. & Wenking, H. Optical detection and fixation of objects by fixed flying flies. *Naturwissenschaften* **56**, 424–425 (1969).
7. Heisenberg, M. & Wolf, R. *Vision in Drosophila: Genetics of Microbehavior* (Springer-Verlag, Berlin, 1984).
8. Reiser, M.B. & Dickinson, M.H. *Drosophila* fly straight by fixating objects in the face of expanding optic flow. *J. Exp. Biol.* **213**, 1771–1781 (2010).
9. Rister, J. *et al.* Dissection of the peripheral motion channel in the visual system of *Drosophila melanogaster*. *Neuron* **56**, 155–170 (2007).
10. Götz, K.G. Visual guidance in *Drosophila*. in *Development and Neurobiology of Drosophila* (eds. Siddiqi, O., Babu, P., Hall, M.L. & Hall, J.C.) 391–407 (Plenum Press, New York, 1980).
11. Strauss, R. & Pichler, J. Persistence of orientation toward a temporarily invisible landmark in *Drosophila melanogaster*. *J. Comp. Physiol. A* **182**, 411–423 (1998).
12. Maimon, G., Straw, A.D. & Dickinson, M.H. A simple vision-based algorithm for decision making in flying *Drosophila*. *Curr. Biol.* **18**, 464–470 (2008).
13. Aptekar, J.W., Shoemaker, P.A. & Frye, M.A. Figure tracking by flies is supported by parallel visual streams. *Curr. Biol.* **22**, 482–487 (2012).
14. Heisenberg, M., Wonneberger, R. & Wolf, R. Optomotor-blind (H31): a *Drosophila* mutant of the lobula plate giant neurons. *J. Comp. Physiol. A* **124**, 287–296 (1978).
15. Geiger, G. & Nässel, D.R. Visual orientation behavior of flies after selective laser beam ablation of interneurones. *Nature* **293**, 398–399 (1981).
16. Hausen, K. & Wehrhahn, C. Neural circuits mediating visual flight control in flies. II. Separation of two control systems by microsurgical brain lesions. *J. Neurosci.* **10**, 351–360 (1990).
17. Bausenwein, B., Wolf, R. & Heisenberg, M. Genetic dissection of optomotor behavior in *Drosophila melanogaster*. Studies on wild-type and the mutant optomotor-blind (H31). *J. Neurogenet.* **3**, 87–109 (1986).
18. Wolf, R. & Heisenberg, M. Visual orientation in motion-blind flies is an operant behavior. *Nature* **323**, 154–156 (1986).
19. Meinertzhagen, I.A. & O'Neil, S.D. Synaptic organization of columnar elements in the lamina of the wild type in *Drosophila melanogaster*. *J. Comp. Neurol.* **305**, 232–263 (1991).
20. Joesch, M., Plett, J., Borst, A. & Reiff, D.F. Response properties of motion-sensitive visual interneurons in the lobula plate of *Drosophila melanogaster*. *Curr. Biol.* **18**, 368–374 (2008).
21. Schnell, B. *et al.* Processing of horizontal optic flow in three visual interneurons of the *Drosophila* brain. *J. Neurophysiol.* **103**, 1646–1657 (2010).
22. Joesch, M., Schnell, B., Raghu, S.V., Reiff, D.F. & Borst, A. ON and OFF pathways in *Drosophila* motion vision. *Nature* **468**, 300–304 (2010).
23. Eichner, H., Joesch, M., Schnell, B., Reiff, D.F. & Borst, A. Internal structure of the fly elementary motion detector. *Neuron* **70**, 1155–1164 (2011).
24. Bausenwein, B. & Fischbach, K. Activity labeling patterns in the medulla of *Drosophila melanogaster* caused by motion stimuli. *Cell Tissue Res.* **270**, 25–35 (1992).
25. Bausenwein, B., Dittrich, A.P. & Fischbach, K.F. The optic lobe of *Drosophila melanogaster*. II. Sorting of retinotopic pathways in the medulla. *Cell Tissue Res.* **267**, 17–28 (1992).
26. Schnell, B., Raghu, S.V., Nern, A. & Borst, A. Columnar cells necessary for motion responses of wide-field visual interneurons in *Drosophila*. *J. Comp. Physiol. A* **198**, 389–395 (2012).
27. Seelig, J.D. *et al.* Two-photon calcium imaging from head-fixed *Drosophila* during optomotor walking behavior. *Nat. Methods* **7**, 535–540 (2010).
28. Brand, A.H. & Perrimon, N. Targeted gene expression as a means of altering cell fates and generating dominant phenotypes. *Development* **118**, 401–415 (1993).
29. Kitamoto, T. Conditional modification of behavior in *Drosophila* by targeted expression of a temperature-sensitive *shibire* allele in defined neurons. *J. Neurobiol.* **47**, 81–92 (2001).
30. Poggio, T. & Reichardt, W. A theory of the pattern induced flight orientation of the fly *Musca domestica*. *Kybernetik* **12**, 185–203 (1973).
31. Wehrhahn, C. Flight torque and lift responses of the housefly (*Musca domestica*) to a single stripe moving in different parts of the visual field. *Biol. Cybern.* **29**, 237–247 (1978).
32. Pick, B. Visual flicker induces orientation behavior in the fly *Musca*. *Z. Naturforsch. C* **29c**, 310–312 (1974).
33. Wehrhahn, C. Fast and slow flight torque responses in flies and their possible role in visual orientation behavior. *Biol. Cybern.* **40**, 213–221 (1981).
34. Reichardt, W. Evaluation of optical motion information by movement detectors. *J. Comp. Physiol. A* **161**, 533–547 (1987).
35. Reichardt, W. & Poggio, T.A. Figure-ground discrimination by relative movement in the visual system of the fly. Part I: Experimental Results. *Biol. Cybern.* **35**, 81–100 (1979).
36. Egelhaaf, M. On the neuronal basis of figure-ground discrimination by relative motion in the visual system of the fly. I. Behavioral constraints imposed on the neuronal network and the role of the optomotor system. *Biol. Cybern.* **52**, 123–140 (1985).
37. Egelhaaf, M. On the neuronal basis of figure-ground discrimination by relative motion in the visual system of the fly. II. Figure-detection cells, a new class of visual interneurones. *Biol. Cybern.* **52**, 195–209 (1985).
38. Liang, P., Heitwerth, J., Kern, R., Kurtz, R. & Egelhaaf, M. Object representation and distance encoding in three-dimensional environments by a neural circuit in the visual system of the blowfly. *J. Neurophysiol.* **107**, 3446–3457 (2012).
39. Egelhaaf, M. On the neuronal basis of figure-ground discrimination by relative motion in the visual system of the fly. III. Possible input circuitries and behavioral significance of the FD cells. *Biol. Cybern.* **52**, 267–280 (1985).
40. Warzecha, A.K., Borst, A. & Egelhaaf, M. Photo-ablation of single neurons in the fly visual system reveals neural circuit for the detection of small moving objects. *Neurosci. Lett.* **141**, 119–122 (1992).
41. Cuntz, H., Haag, J. & Borst, A. Neural image processing by dendritic networks. *Proc. Natl. Acad. Sci. USA* **100**, 11082–11085 (2003).
42. Borst, A. *Drosophila*'s view on insect vision. *Curr. Biol.* **19**, R36–R47 (2009).

ONLINE METHODS

Behavioral experiments. The locomotion recorder[2,27] consisted of an air-suspended sphere floating in a bowl-shaped sphere holder. The sphere had a diameter of 6 mm and a weight of 40 mg; it was made from polyurethane foam and coated with polyurethane spray (spheres were kindly provided by V. Jayaraman, Janelia Farm). The airflow is adjusted to ~0.7 l min^{-1} by a rotary vane pump (G6/01-K-EB9L Gardner Denver Thomas GmbH) such that the sphere rotated freely in the holder, but did not jump out. A high-power infrared LED (800 nm, JET series, 90 mW, Roithner Electronics) was located in the back to illuminate the fly and the sphere surface. Two optical tracking sensors were equipped with lens and aperture systems to focus two 1-mm^2 equatorial spots (at ±30°) on the sphere at a distance 15 cm behind the fly. The tracking data were processed in a custom-designed circuit[27] at 4 kHz internally, read out via a USB interface and processed by a computer at ~200 Hz. This allowed real-time calculation of the instantaneous rotation axis of the sphere. A third camera (GRAS-20S4M-C, Point Grey Research) was located in the back, which is essential for proper positioning of the fly and allowed real-time observation and video recording of the fly during experiments. The bottom of the sphere holder was surrounded by an open plastic funnel connected to a metal fan with an aluminum tube. A self-designed Peltier controlling system read out the temperature of a thermometer placed just below the sphere and controlled the fan temperature such that the air temperature around the fly was regulated precisely (±0.1 °C). In all experiments, the temperature started at the permissive temperature level for *shibire^{ts}* (25 °C) and was raised linearly to the restrictive temperature of 34 °C in 10–20 min. Three 120-Hz LCD screens (Samsung 2233 RZ) were vertically arranged and formed a U-shaped visual arena (31 × 31 × 47 cm) with the fly in the center. We removed the monitor covers to minimize the borders between the screens in the corners of the arena and glued thin sheets of parchment paper onto the screens to scatter and evenly distribute the emitted light. The visual arena had a luminance ranging from 0–131 cd m^{-2} and covered almost the whole visual field of the fly (horizontal, ± 135°; vertical, ± 57°; resolution < 0.1°). The three LCD screens were controlled via NVIDIA 3D Vision Surround Technology on Windows 7 64 bit, allowing a synchronized update of the screens at 120 frames per s. For visual stimulation, we use Panda3D, an open-source gaming engine, and Python 2.7, which simultaneously controlled the frame rendering in Panda3D, read out the tracking data and temperature, and streamed data to the hard disk.

Time-position plots for the visual stimuli are illustrated in **Supplementary Figure 4** for all experiments. The large-field open-loop optomotor stimulus (**Fig. 1b–d** and **Supplementary Fig. 4a**,**b**) consisted of a striped grating (λ = 20°) rotating clockwise (+) or counterclockwise (−) at a velocity of 20 ° s^{-1} for 0.5 s. Seven contrasts were tested. The dark stripes always had a luminance value of 27 cd m^{-2}, whereas the luminance values of the brighter stripes ranged from 30–104 cd m^{-2}, resulting in contrast values between 4 and 58%, measured as $(I_{max}-I_{min})/(I_{max}+I_{min})$. In the open- and closed-loop fixation experiments, we showed a single black bar (10° wide, 114° high, 9 cd m^{-2}) on a gray background (58 cd m^{-2}). In the first set of open-loop fixation experiments (**Fig. 2** and **Supplementary Fig. 4d**,**e**), the bar started in the back and rotated at velocities of ±18 ° s^{-1} around the fly. In another set of experiments (**Fig. 3** and **Supplementary Fig. 4f**), the bar did not move, but slowly appeared (in 0.5 s), remained static for 4 s and disappeared (in 0.5 s) at well-defined locations (±120°, ±90°, ±60°, ±45°, ±30° and ±15°). In another experiment (**Fig. 4** and **Supplementary Fig. 4g–i**), we chose two locations (Ψ = 30° and Ψ = 60°) to show local motion (front to back and back to front) and local luminance change. Here, the local luminance change dynamics were chosen such that they approximated the luminance change when the local motion was shown. In the case of closed-loop fixation, the bar was placed at a random position (between −180° and +180°) around the fly before each trial and the fly was then given 20 s control of the angular position of that bar (Δbar = −fly turning, updated approximately every 9 ms). This was done either in front of a gray background (**Fig. 1e–i** and **Supplementary Figs. 3a–c** and **4c**) or a large-field sine-grating (λ = 30°, the luminance values of the pattern were between 27 and 104 cd m^{-2}). The sine-grating was either static (**Supplementary Figs. 3d–f** and **4j**) or rotated at ±15 ° s^{-1} (**Fig. 5** and **Supplementary Fig. 4k**,**l**).

Flies were raised on standard cornmeal-agar medium at 18 °C and 60% humidity throughout development on a 12-h light, 12-h dark cycle. We used *shi^{ts}* control flies (*w^+; +; +/UAS-shi^{ts}*), T4/T5 control flies (*w^+/w^-; +; R42F06-Gal4/+*) and T4/T5 block flies (*w^+/w^-; +; R42F06-Gal4/UAS-shi^{ts}*). The T4 and T5 cell–specific driver line *R42F06-Gal4* was kindly provided by A. Nern and G. Rubin (Janelia Farm) and was generated[43] using a 4.0-kb DNA fragment of the *bab2* gene amplified from genomic DNA with primers CGGCTGATCCAACAAAGGATG CACC and CTCAGTGTAGCCGCACCTTGTTCCT. The *shibire^{ts}* effector has multiple insertions on the third chromosome. We used wild-type Canton S flies for the control crosses. Only female flies aged 2–10 d were used in experiments. Flies were taken from 18 °C just before the experiment and immediately cold anesthetized. The head, thorax and wings were glued to a needle using near-ultraviolet bonding glue (Sinfony Opaque Dentin) and strong blue LED light (440 nm, dental curing light, New Woodpecker).

For each fly, the experiment lasted approximately 50 min and was split into 50–200 trials depending on the length and the number of visual stimuli. Stimuli in one trial were presented in random order. For data analysis, we chose a range of trials (same for control and T4/T5 block flies per experiment) during which the temperature was constant at 34 °C and during which flies had a constant average turning and walking speed. The experimental raw data were first downsampled (interpolated from 120 to 20 Hz). Turning speed traces were then determined by taking the average over trials and low-pass filtering the resulting trace (τ = 0.1 s in all experiments, except those shown in **Fig. 2**, where τ = 0.4 s). Probability density functions of bar position were calculated separately for each trial with a bin size of 5° and then averaged over trials and flies. The measure 'fixation in front' was determined by integrating the probability density function of one trial between −10° and 10°, which resulted in a percentage value for how probable it was to find the bar in that area during that trial. These values were then averaged over trials and flies. Flies were excluded from data analysis when the average walking speed during the whole experiment was below 0.1 cm s^{-1}, indicating severe walking problems, or (only in closed-loop fixation experiments with static background) when the average turning speed was either larger than +10 ° s^{-1} or smaller than −10 ° s^{-1}, indicating an asymmetry in walking behavior that led to a substantially reduced fixation performance. All data analysis was performed in Python 2.7 using NumPy and SciPy on Mac OSX 10.8.

P values were obtained using different statistical tests. To test the hypothesis that a group had a certain mean, we performed a two-sided *t* test. When two groups were compared (**Fig. 4k**), we performed a two-sided *t* test. When T4/T5 block flies were compared with *shi^{ts}* control and T4/T5 control flies, we performed a two-sided *t* test comparing each control with the block flies and chose the larger *P* value. When three groups were compared (**Fig. 4j**), we performed a one-way ANOVA. We used approximately the same sample size (smallest n = 9 flies, largest n = 16 flies) per group and experiment, which permitted a statistical comparison between the different experiments. This sample size was considered as sufficiently large because the optomotor response of T4/T5 block flies shown in **Figure 1b–d** was highly significantly reduced at n = 10 flies (P < 0.001, two-sided *t* test compared with both controls). See **Supplementary Statistics** for a detailed list of group sizes, statistical tests and *P* values.

Electrophysiology. Patch-clamp recordings were performed as described previously[20] with minor modifications. All electrophysiological experiments were performed with female wild-type Canton S flies 6–24 h post-eclosion. Flies were raised on standard cornmeal-agar medium and kept at 25 °C and 60% humidity on a 12-h dark/light cycle.

Flies were anesthetized on ice and immobilized on a plexiglas holder with wax. The head was bent downwards and fixed by waxing the proboscis to the thorax. The fly was then inserted into an opening cut into a piece of aluminum foil mounted in a recording chamber. A part of the posterior side of the head cuticle and the muscle that covers the cell bodies of LPTCs was removed with fine forceps. Extracellular saline (103 mM NaCl, 3 mM KCl, 5 mM TES, 10 mM trehalose, 10 mM glucose, 7 mM sucrose, 26 mM $NaHCO_3$, 1 mM NaH_2PO_4, 1.5 mM $CaCl_2$ and 4 mM $MgCl_2$, pH 7.3, 280 mOsm) was bubbled with 95% O_2 and 5% CO_2 and continuously perfused over the preparation. The brain of the fly was visualized with an upright microscope (Axiotech Vario 100, Zeiss) equipped with a 40× water-immersion objective (LumPlanFL, NA 0.8, Olympus) and an Hg-light source (HXP-120, Visitron Systems). For contrast enhancement, we used two polarization filters that were slightly shifted with respect to their polarization plane. The health of the flies was checked regularly by monitoring periodic movements of the brain. A glass electrode filled with collagenase (Collagenase IV, Gibco, 0.5 mg ml^{-1} in extracellular saline) was used to weaken the perineural sheath and expose the somata of LPTCs.

Somata of vertical system and horizontal system cells were patched with a glass electrode (6–9 MΩ) filled with internal solution (140 mM potassium aspartate, 10 mM HEPES, 4mM Mg-ATP, 0.5 mM Na-GTP, 1 mM EGTA, 1 mM KCl and 0.03 mM Alexa 568–hydrazide sodium, pH 7.26, 265 mOsm). All recordings were performed in current-clamp bridge mode with an NPI BA-1S amplifier (NPI electronics), low-pass filtered at 3 kHz and digitized at 10 kHz. Data acquisition was performed with Matlab (version R2011a, MathWorks). Cells had an average resting membrane potential of −51.6 ± 0.7 mV (corrected for a liquid junction potential of 12 mV) and an average input resistance of 204.5 ± 16.7 MΩ. Cell types were identified on the basis of their typical response profiles to moving gratings. In addition, fluorescence images of each cell were taken after the recording with a CCD camera (Spot Pursuit, Visitron Systems) to verify their identity.

Visual stimuli were presented on a custom-built LED arena that subtended 170° in azimuth and 85° in elevation with a resolution of approximately 1.4° per LED. The arena allowed refresh rates of up to 600 Hz and had a maximum luminance of 80 cd m^{-2}. Motion stimuli consisted of square-wave gratings with a wavelength of 20° moving at 1 Hz. Stimuli lasted for 3 s with an interstimulus interval of 5 s and were repeated three times. For bar flicker stimuli, the arena background was set to full luminance. After 1.5 s, a dark bar that had a width of 10° and was centered at 30°, 60° or 90° along the azimuth appeared. The contrast of that bar was increased linearly to a maximum of 66% over 0.5 s or 1.5 s. After an interval of 3 s, the dark bar disappeared again in the same time period. Bar flicker stimuli were presented five times. For full-field flicker stimuli, the arena was stepped to full luminance for 3 s and then back to zero again for 3 s. Full-field flicker stimuli were presented ten times per cell.

Data analysis was performed with Matlab (version R2011b, MathWorks) using custom-written scripts. For all stimuli, we averaged voltage traces over sweeps and calculated the mean and s.e.m. over cells. The baseline membrane potential was calculated by averaging over a period of 500 ms preceding the stimulus onset and subtracted from the responses. For horizontal system cells, we pooled responses of all three horizontal system cell types. To properly match the receptive field of vertical system cells[20], we averaged the responses of vertical system cells with frontal receptive fields (VS1–VS3) to obtain the responses to the appearing and disappearing bar at 30° and 60°. Responses of vertical system cells with lateral receptive fields (VS5–6) were averaged to determine the responses at 90°.

Modeling. Visual patterns were modeled as one-dimensional luminance functions at a spatial resolution of 0.01° and a temporal resolution of 1 ms. They were covered by 360 elementary motion detectors of the Reichardt type[34]. Briefly, the luminance value at one location was low-pass filtered (first-order, 20-ms time constant) and subsequently multiplied with the instantaneous value derived from the neighboring location, separated by 1° of visual angle. This was done twice in a mirror-symmetrical fashion, and the output signals of both operations were subtracted. All elementary motion detectors were weighted according to the $M(\Psi)$ sensitivity profile and subsequently summated. In each hemisphere, motion detection subunits tuned to back-to-front motion were given half the response amplitude of those tuned to front-to-back motion. The visual pattern was also viewed by an array of 360 position detectors. These were modeled as high-pass filters (first-order, 10-ms time constant), the outputs of which were squared. From this array, the location of the maximum was determined. If this maximum was below a certain threshold, the location decayed back to zero with a 20-ms time constant. The output of the position system was calculated as the value of the $P(\Psi)$ function at this location. The $M(\Psi)$ and $P(\Psi)$ functions were approximated in the following way, with $Z(\Psi)$ describing the shape of their profiles, g_P being the gain factor of the position system (= 3) and g_M being the gain factor of the motion system (= 5).

$$Z(\Psi) = -\frac{d}{d\Psi} e^{-(\Psi/75)^2}$$
$$P(\Psi) = g_P \cdot Z(\Psi)$$
$$M(\Psi) = g_M \cdot |Z(\Psi)|$$

$M(\Psi)$ was subsequently smoothed by a box filter of 20° width. As a noise function we used Gaussian white noise that was filtered by a first-order low-pass filter with 100-ms time constant and multiplied with a noise-gain factor (g_N = 15). The sum of noise, motion and position system was then fed through a first-order low-pass filter with 100-ms time-constant to result in the turning speed. In closed-loop simulations, the turning speed was used to update the bar position each millisecond.

$$\text{bar position}(t+1) = \text{bar position}(t) - 0.1 \cdot \text{turning speed}(t)$$

Fixation histograms were obtained from 20 simulation runs, each 30 s long. At the beginning of each run, the bar was positioned in front of the fly. As large field pattern, we used a sine-grating with a spatial wavelength of 22.5°, a mean luminance of 0.5 and a contrast of 1. When activated, it moved at 10 ° s^{-1}, resulting in a temporal frequency of 0.44 Hz. The black bar was simulated as zero luminance from −5° to + 5° around the bar location, replacing the luminance value of either the grating or the one of a uniform background of luminance value 1. The model was simulated in IDL (Exelis) on 64-bit Windows 7.

43. Pfeiffer, B.D. *et al.* Tools for neuroanatomy and neurogenetics in *Drosophila*. *Proc. Natl. Acad. Sci. USA* **105**, 9715–9720 (2008).